

Finite Element Studies of Homogeneous and Heterogeneous Dislocation Nucleation based on the Rice-Peierls Framework

T.L. Li,¹ J.H. Lee,² Y.F. Gao,^{1,3}

¹ Department of Materials Science and Engineering, University of Tennessee, Knoxville, TN 37996, U.S.A.

² Division for Research Reactor, Korea Atomic Energy Research Institute, Daejeon 305-353, Republic of Korea

³ Computer Science and Mathematics Division, Oak Ridge National Laboratory, Oak Ridge, TN 37831, U.S.A.

ABSTRACT

The study of dislocation nucleation has gained increasing attentions recently primarily due to the advancement of small scale mechanical testing methods. Based on the classic Rice model of dislocation nucleation from a crack tip in which the dislocation core is modeled by a continuous slip field, a nonlinear finite element method can be formulated with the interplanar potential as the input, and the development of interplanar slip field can be solved from the resulting boundary value problems. The effects of geometric boundary conditions, loading patterns, etc. can be conveniently determined, as opposed to the time consuming molecular simulations. To validate the method, we compare the simulations results of homogeneous dislocation nucleation and heterogeneous dislocation nucleation from a two-dimensional crack tip to the literature results. As proposed by Rice and Beltz (J. Mech. Phys. Solids, 1994), the activation energy for dislocation nucleation from a three-dimensional crack tip depends on the finite thickness in the direction parallel to the crack tip, which has been successfully reproduced in the finite element simulation results reported here.

INTRODUCTION

With the rapid development of micro- and nano-scale material structures and small scale mechanical testing methods, the study of dislocation nucleation has gained increasing attentions recently. Examples include the homogeneous dislocation nucleation under indentation (thus leading to the pop-in behavior on the load-displacement curves) [1-5] and heterogeneous dislocation nucleation from sharp features in strained nano-electronics [6-10]. A dislocation is usually modeled either by the Volterra model [11-13], which treats the dislocation as a mathematical discontinuity, or by the Peierls-Nabarro model, which treats the dislocation core as a continuous slip field [14-18]. Based on the diffused-core model, dislocation nucleation from stress concentration sites such as a crack tip is viewed as a gradual development of the interplanar slip field until an instability is reached [14,15].

The relative slip between two adjacent layers of the slip plane, Δ_α , and the shear stress on the slip plane, τ_α , are related through $\tau_\alpha = \partial\Phi/\partial\Delta_\alpha$, where $\Phi(\Delta_\alpha)$ is a periodic interplanar potential and is also denoted as the γ surface, and $\alpha = 1, 2$ are the two slip directions on the slip plane [14,15]. The total potential energy Π is

$$\Pi = \Pi_0 + \int_S \Phi(\Delta) dS + \frac{1}{2} \int_S \mathbf{n} \cdot \tilde{\boldsymbol{\sigma}} \cdot \Delta dS - \int_S \mathbf{n} \cdot \boldsymbol{\sigma}^{elastic} \cdot \Delta dS, \quad (1)$$

where \mathbf{n} denotes the slip plane normal, $\tilde{\boldsymbol{\sigma}}$ is the self stress due to a non-uniform Δ when the applied load is zero, and $\boldsymbol{\sigma}^{elastic}$ is the elastic stress fields when $\Delta = 0$ (i.e., when there is no slip field). The dislocation will be nucleated when the total potential energy reaches a stationary point. The resulting boundary value problem from the Rice-Peierls model can be numerically solved by ad hoc methods such as collocation method to solve the Cauchy integral equation [15] or the variational boundary integral method [16-18]. In analogy to the cohesive interface model [19], the above formulation has been implemented into a commercial finite element package, ABAQUS, via a User-defined ELEMENT (UEL) subroutine [20]. The surrounding continuum elements are either eight-node brick element (C3D8) in 3D model or four-node plane strain element (CPE4) in 2D model, so that the interface elements are made of either eight or four nodes. We find the relative slip field on the slip plane by balancing the force introduced from our cohesive interface model and the applied force. The advantage of using finite element method is that it can solve more complex problems, and it costs less computation time when compared to molecular simulations [21,22], although important atomistic aspects such as nonlocal interaction may not be well captured.

Dislocation nucleation is a stress-assisted, thermally activated process. When the applied load is less than but close to the critical load, the dislocation nucleation may still occur due to the thermal energy that overcomes the nucleation energy barrier. Under this condition, there are two solutions of the slip field for the same applied load – one corresponding to the minimum potential energy, $\Delta_\alpha^{min}(x, y)$, and the other being a saddle point configuration, $\Delta_\alpha^{saddle}(x, y)$. The activation energy can be calculated from

$$\Delta\Pi = \Pi[\Delta_\alpha^{saddle}(x, y)] - \Pi[\Delta_\alpha^{min}(x, y)]. \quad (2)$$

To obtain the saddle point solution, an initial trial function of $\Delta_\alpha^{saddle}(x, y)$ is prescribed on the slip plane. If this guess is near the saddle point solution, the Newton-Raphson iteration, in this case, will quickly converge to the saddle point solution

HOMOGENEOUS DISLOCATION NUCLEATION

Consider an infinite solid under pure shear stress. Our three-dimensional finite element model is shown in Fig. 1(a) where a half model is used because of symmetry about the x - z plane. The shear stress on the slip plane is taken to be a Frenkel sinusoidal function of the relative slip across the slip plane,

$$\tau_\alpha = \tau_{max} \sin\left(\frac{2\pi\Delta_\alpha^*}{b}\right), \quad (3)$$

$$\Delta_\alpha = \Delta_\alpha^* - \frac{b}{2\pi} \sin\left(\frac{2\pi\Delta_\alpha^*}{b}\right), \quad (4)$$

where τ_{max} the interface theoretical strength in shear, and b is the magnitude of Burgers vector. The relationship in Eq. (4) is introduced so that the initial slope of $\tau_\alpha \sim \Delta_\alpha$ is infinite, thus denoted as slanted model. The saddle point solutions of the slip field, Δ_x^{saddle} , on the slip plane are

given in Figs. 1(b) and 1(c). The inhomogeneous slip field in Fig. 1(b) at lower stress has a larger size than that in Fig. 1(c).

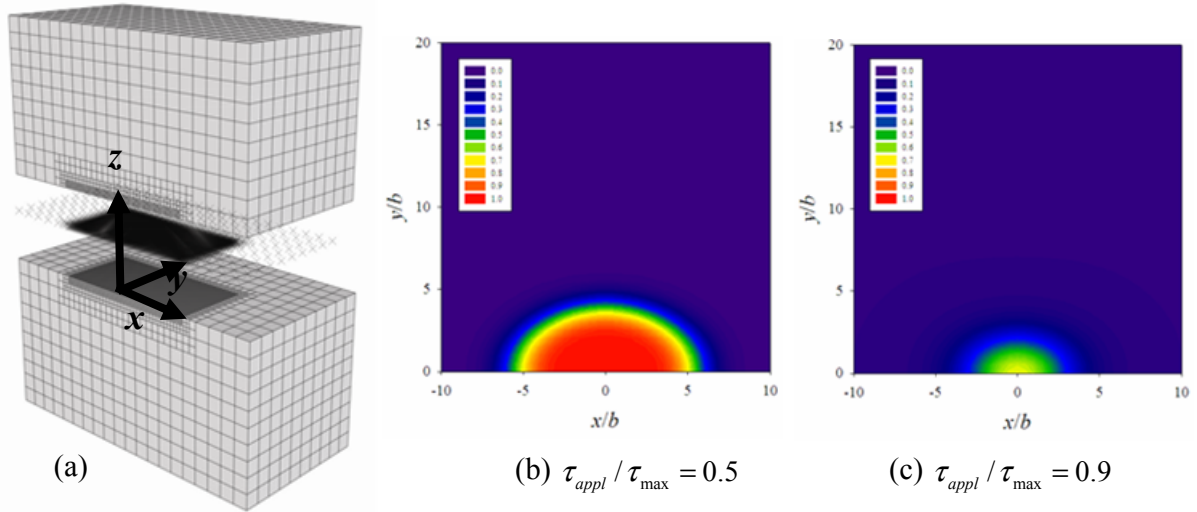


Figure 1. (a) The three-dimensional finite element model for the study of homogeneous dislocation nucleation under pure shear stress. (b) and (c) The saddle point solutions of the relative slip distribution along the shear direction with respect to two stress levels.

Fig. 2(a) presents the 3D activation energy (i.e., $\Delta\Pi^{3D}$) for the homogeneous dislocation nucleation calculations in Fig. 1, where μ and ν are shear modulus and Poisson's ratio, respectively. The smaller the applied stress is, the larger the activation energy of dislocation nucleation will be. Predictions in Fig. 2(a) agree favorably with molecular simulations [23] in terms of the dependence on μb^3 and crystal structure.

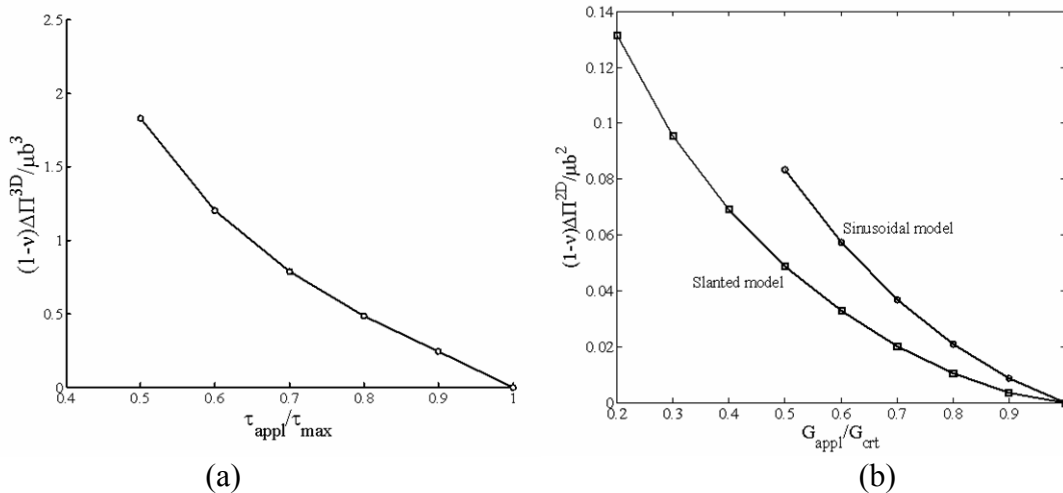


Figure 2. (a) The activation energy for homogeneous dislocation nucleation, $\Delta\Pi^{3D}$ normalized by $\mu b^3 / (1-\nu)$, as a function of various applied pure-shear stress levels. (b) The activation energy per unit length, $\Delta\Pi^{2D}$, for dislocation nucleation from a two-dimensional crack tip using the slanted and simple sinusoidal models.

HETEROGENEOUS DISLOCATION NUCLEATION FROM A CRACK TIP

Consider a half infinite crack with dislocation emitted onto a coplanar slip plane under the applied K field in Fig. 3(a). We focus on the edge dislocation nucleation under Mode II load. According to Rice and Beltz [15], the dislocation is nucleated from the crack tip when the applied energy release rate G_{appl} reaches G_{crit} (e.g., $G_{crit} = \tau_{max} b / \pi$ in Frenkel model). We first conduct simulations under 2D condition. In this case, the activation energy $\Delta\Pi^{2D}$ is given in terms of unit length in the third direction. We compare our results that use slanted model in the cohesive plane to those using the simple sinusoidal model. It is seen that the simple sinusoidal model has larger activation energy than the slanted model at the same applied load level due to the additional compliance in the simple sinusoidal model. Our 3D finite element model is shown in Fig. 3(b) with a finite thickness of H . The slip direction is along the x direction. Symmetry is used on the surface $Z = 0$ and the normal displacements on the outside surface (i.e. $Z = -H$) are fixed to ensure a plane strain condition.

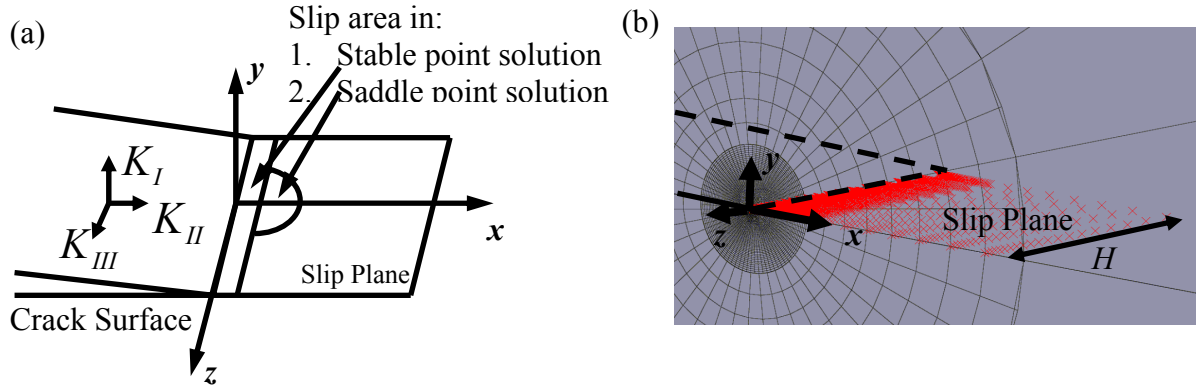


Figure 3. (a) A planar crack under the mixed-mode k -field. The relative slip occurs on the x - z plane. (b) Dislocation nucleation from the planar crack tip under mode II load.

The saddle point configurations are shown in Fig. 4 for $G_{appl} / G_{crit} = 0.9$ and 0.7 , respectively, which resemble half dislocation loops. Similar to the homogeneous dislocation nucleation, a large applied load corresponds to a large size of the saddle point distribution. We also examine another prediction by Rice and Beltz [15]. In their work, they use the asymptotic method to obtain an approximate saddle point solution, consisting of a local protrusion of a dislocation loop. They argued that the activation energy, $\Delta\Pi^{3D}$, for three-dimensional dislocation nucleation varies with the model thickness H in Fig. 3b and is close to the product of $\Delta\Pi^{2D}$ and H (i.e. $\Delta\Pi^{3D} \approx H\Delta\Pi^{2D}$) when H is small, because the small thickness does not allow the development of the local protrusion in the thickness direction and thus force the saddle-point solution to be independent of z . And $\Delta\Pi^{3D}$ should reach a plateau as H increases. They calculated a case when the applied energy release rate is close to the critical value (i.e., $G_{appl} / G_{crit} = 0.9$) where their asymptotic approximation is most reliable, and found out that $H\Delta U^{2D}$ agrees with the actual $\Delta\Pi^{3D}$ up to H about $17b$. We verify their prediction in Fig. 4(c).

Three-dimensional activation energies at $G_{\text{appl}} / G_{\text{crt}} = 0.9$ and 0.7 are given as a function of thickness H/b . $H\Delta\Pi^{2D}$ is plotted as solid lines to compare with the 3D results. Our results exhibit the same trend as that predicted by Rice and Beltz. In our simulations, $H\Delta\Pi^{2D}$ is close to $\Delta\Pi^{3D}$ until H reaches about $13b$.

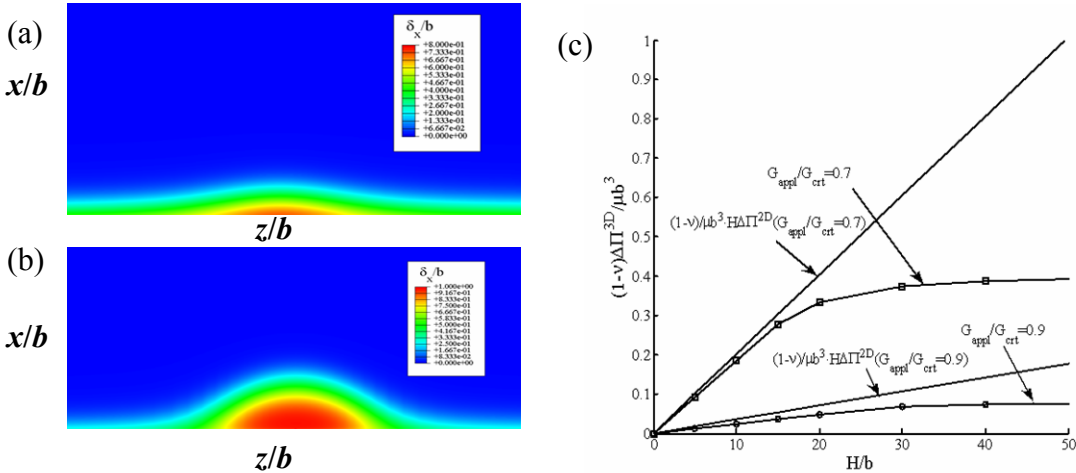


Figure 4. The saddle point solutions of the slip field when the applied energy release rate is (a) $G_{\text{appl}} / G_{\text{crt}} = 0.9$ (b) $G_{\text{appl}} / G_{\text{crt}} = 0.7$. (c) The normalized activation energy $\Delta\Pi^{3D}$ under applied stress levels $G_{\text{applied}} / G_{\text{crt}} = 0.9$ (i.e., solid line marked with circles) and $G_{\text{applied}} / G_{\text{crt}} = 0.7$ (i.e., solid line marked with squares) as a function of the normalized H/b . The product of normalized $\Delta\Pi^{2D}$ (in Fig. 3(b)) and thickness H is also shown for comparison.

SUMMARY

Several applications of a finite element formulation of the Rice-Peierls framework have been demonstrated in homogeneous dislocation nucleation and heterogeneous dislocation nucleation from a crack tip. Geometric boundary effects can be conveniently studied in this methodology. We have verified the proposed relationship in [15] between the activation energy and the calculation size. These results may help design appropriate sizes in molecular simulations.

ACKNOWLEDGEMENTS

Financial support for this work was provided by the NSF CMMI 0900027 and by the Materials Sciences and Engineering Division, Office of Basic Energy Sciences, US Department of Energy.

REFERENCES

1. T.F. Page, W.C. Oliver, and C.J. McHargue, *J. Mater. Res.* **7**,450 (1992).
2. C.A. Schuh, J.K. Mason, and A.C. Lund, *Nat. Mater.* **4**, 617 (2005).
3. A.H.W. Ngan, L. Zuo, and P.C. Wo, *Proc. R. Soc. A* **462**, 1661 (2006).
4. H. Bei, Y.F. Gao, S. Shim, E.P. George, and G.M. Pharr, *Phys. Rev. B* **77**, 060103 (2008).

5. T.L. Li, Y.F. Gao, H. Bei, and E.P. George, *J. Mech. Phys. Solids.*, **59**, 1147 (2011).
6. M. Kammler, D. Chidambarrao, K.W. Schwarz, C.T. Black, and F.M. Ross, *Appl. Phys. Lett.* **87**, 133116 (2005).
7. Z. Zhang, J. Yoon, and Z. Suo, *Appl. Phys. Lett.* **89**, 261912 (2006).
8. M. Feron, Z. Zhang, and Z. Suo, *J. Appl. Phys.* **102**, 023502 (2007).
9. T.L. Li, J.H. Lee, Y.F. Gao, G.M. Pharr, M. Huang, and T.Y. Tsui, *Appl. Phys. Lett.* **96**, 171905 (2009).
10. J.H. Lee, Y.F. Gao, *Int. J. Solids Struct.* **48**, 1180 (2011).
11. J.P. Hirth and J. Lothe, *Theory of Dislocations*, Krieger, New York (1982).
12. T.Y. Zhang and J.C.M. Li, *Mater. Sci. Eng. A* **142**, 36 (1991).
13. J.R. Rice and R. Thomson, *Phil. Mag.* **29**, 73 (1973).
14. J.R. Rice, *J. Mech. Phys. Solids.* **40**, 239 (1992)
15. J.R. Rice and G.E. Beltz, *J. Mech. Phys. Solids.* **42**, 333 (1994).
16. G. Xu, A.S. Argon and M. Ortiz, *Philos. Mag. A.* **72**, 415 (1995).
17. G. Xu and A.S. Argon, *Phil. Mag. Lett.* **80**, 605 (2000).
18. G. Liu and G. Xu, *J. Mech. Phys. Solids.* **57**, 1078 (2009).
19. Y.F. Gao and A.F. Bower, *Modelling Simul. Mater. Sci. Eng.* **12**, 453 (2004).
20. Y.F. Gao, *J. Mech. Phys. Solids.*, **58**, 2023 (2010).
21. T. Zhu, J. Li, and S. Yip, *Phys. Rev. Lett.* **93**, 025503 (2004).
22. S. Izumi and S. Yip, *J. Appl. Phys.* **104**, 033513 (2008).
23. H.A. Saeed, S. Izumi, S. Hara, S. Sakai, *Mater. Res. Soc. Symp. Proc.* **1297**, 105 (2011).